Preprints.org

Article

An Insight Into the Inhibitory Mechanisms of Hesperidin on α-Glucosidase Through Kinetics, Fluorescence Quenching and Molecular Docking Studies

Kumaravel Kaliaperumal , Linyan Zhang , Liangliang Gao , Qin Xiong , Yan Liang , Yueming Jiang , Jun Zhang *

Article

An Insight into the Inhibitory Mechanisms of Hesperidin on α-Glucosidase through Kinetics, Fluorescence Quenching and Molecular Docking Studies

Kumaravel Kaliaperumal [1,2,†], Linyan Zhang [1,†], Liangliang Gao [1], Qin Xiong [1], Yan Liang [1], Yueming Jiang [1,3] and Jun Zhang [1,*]

[1] National Engineering Research Center of Navel Orange, Gannan Normal University, Ganzhou 341000, China; kumarbio06@gmail.com (K.K.); 15899824665@139.com (L.Z.); togaoliangliang@outlook.com (L.G.); skyxiongqin@163.com (Q.X.); zjhxy110@126.com (Y.L.); ymjiang@scbg.ac.cn (Y.J.)

[2] Unit of Biomaterials Research, Department of Orthodontics, Saveetha Dental College, Saveetha University, SIMATS, Chennai, Tamil Nadu, India

[3] South China Botanical Garden, Chinese Academy of Science, Guangzhou 510650, China

* Correspondence: bri71527152@outlook.com

† Equal contribution to this work.

Abstract: The α-glucosidase inhibitor is of interest to researchers due to its association with type-II diabetes treatment by suppressing postprandial hyperglycemia. Hesperidin is a major flavonoid in orange fruit with diverse biological properties. This paper evaluates the effects of hesperidin on α-glucosidase through inhibitory kinetics, fluorescence quenching, and molecular docking methods for the first time. The inhibition kinetic analysis showed that hesperidin reversibly inhibited the α-glucosidase activity with an IC$_{50}$ value of 18.52 µM and the inhibition was performed in an uncompetitive type. Fluorescence quenching studies indicated that the intrinsic fluorescence of α-glucosidase was quenched via a static quenching process and only one binding site was present between hesperidin and α-glucosidase. The interaction between them was spontaneous and mainly driven by hydrogen bonds as well as hydrophobic forces. Furthermore, molecular docking results suggested that hesperidin might bond to the entrance or outlet part of the active site of α-glucosidase through a network of five hydrogen bonds formed between hesperidin and the four amino acid residues (Trp709, Arg422, Asn424, and Arg467) of α-glucosidase and hydrophobic effects. These results provide new insights into the inhibitory mechanisms of hesperidin on α-glucosidase, supporting the potential application of hesperidin-rich orange product as a hypoglycemic functional food.

Keywords: hesperidin; α-glucosidase; antidiabetic; flavonoid; orange

1. Introduction

Diabetes mellitus (DM) is a metabolic illness presently influencing 425 million individuals around the world and the overall number is assessed to be 642 million in 2045 [1]. DM is frequently accompanied by extreme complications, including cardiovascular infections, neuropathy, retinopathy, and kidney disappointment [2]. As the foremost common sort of DM, type II diabetes is recognized as having a close relationship with the occurrence of postprandial blood glucose [3]. In this manner, appropriate control of postprandial hyperglycemia is exceptionally essential for the control of type II diabetes.

α-glucosidase is an important catabolic enzyme that engages in the decomposition of oligosaccharides into monosaccharides. The glucose produced from starch by α-glucosidase-

catalyzed decomposition is quickly assimilated into the blood, causing the occurrence of high levels of postprandial blood glucose [4]. Hence, α-glucosidase is specifically related to type II diabetes, and the retardation of the enzymatic activity of α-glucosidase might diminish the postprandial glucose levels, which could be an efficient treatment for type II diabetes. Plenty of investigations have been carried out previously, trying to discover the efficient inhibitors of α-glucosidase to manage the diabetes [5]. Although famous synthetic medicines for type II diabetes treatment, like acarbose, metformin, and miglitol, are efficient α-glucosidase inhibitors, they are found to have serious side effects, such as hepatotoxicity and adverse gastrointestinal symptoms [3,5]. Therefore, it is of much interest to search for alternative antidiabetic modulator without any adverse effects on the health system. Natural resources such as traditional herbs and functional fruits, are abundant with biologically interesting compounds, which have been widely explored for the development of naturally occurring inhibitors on α-glucosidase. For example, narcissoside isolated from *Anoectochilus roxburghii* [6], trilobatin obtained from *Lithocarpus polystachyu* [7], and prenylated flavonoids isolated from Mulberry Leaves [8], are reported to exhibit excellent inhibitory effect on α-glucosidase, showing high application potential as natural antidiabetic agents.

Hesperidin, a flavonoid glycoside, is predominant in citrus fruits like orange, lemon, and grapefruit. Hesperidin is a natural plant defense molecule that protects the host plant against pest and microbial infections [9]. Apart from these, hesperidin has many biomedical properties like anticancer, anticoagulant, antioxidant, and cardioprotection effects [10–12]. Hesperidin is found abundant in both juice and peel of orange fruits. For example, Gannan navel orange juice contains over 250 mg/L of hesperidin [13]; Orange peels are reported to have high hesperidin content, being about 42.56 mg per gram of dry weight of 95% ethanolic extract [14]. In most of the orange juice processing industries, the orange peel is discarded as byproduct wastes without recovering its hesperidin and other valuable products. Despite various biological effects that hesperidin possesses, the antidiabetic effect of hesperidin in lowering the blood glucose levels has still not validated [15]. Previous studies reveal that hesperidin exhibits a considerable inhibitory effect against α-glucosidase [16,17], however, the inhibitory mechanism remains unknown, which greatly restricts its further application for the management of diabetes. In the present study, the inhibitory effect and the action mode of hesperidin binding to α-glucosidase were investigated through in vitro enzyme kinetics, fluorescence quenching assay, and molecular docking studies for the first time. The results revealed here might shed light on the inhibitory mechanism of hesperidin on α-glucosidase, thereby greatly benefiting the application potential of hesperidin-rich orange products like orange juice and orange peel as natural hypoglycemic agents.

2. Materials and Methods

2.1. Chemicals and Instruments

Hesperidin was obtained commercially from Shanghai Yuanye Biotechnology Company (Yuanye, Shanghai, China). α-glucosidase (EC 3.2.1.20, from *Saccharomyces cerevisiae*) was purchased from Sigma-Aldrich Chemical. (St. Louis, MO, USA). Acarbose and *p*-nitrophenyl-α-D-glucopyranoside (*p*NPG) were purchased from Aladdin Industrial Corporation (Shanghai, China). De-ionized water was obtained from a Milli-Q Gradient A10 system (Millipore, Billerica, USA). All other chemicals and solvents were of analytical grade and purchased from Damao Chemical Reagent Factory (Tianjin, China). A microplate reader (Tecan Spark 10M, Männedorf, Switzerland) was employed for the UV absorbance measurements. Fluorescence intensity was measured by using a fluorescence spectrophotometer (F-7000; Hitachi High-Tech Science Co., Japan).

2.2. In Vitro α-Glucosidase Inhibition Assay

α-Glucosidase inhibition assay was carried out using a previous procedure with slight modifications [17]. In brief, to the wells of a 96-well microplate, α-glucosidase (50 μL, 0.185 U/mL) and phosphate buffer (40 μL, pH 6.8) were added, followed by the addition of hesperidin (20 μL) with various concentrations from 5 to 125 μg/mL. The reaction mixture was shaken well and

incubated at 37 °C for 10 min. After that, 4 mM *p*NPG (50 μL) was added to the incubating reaction mixture as a substrate to trigger the enzymatic reaction, and the absorbance of the mixture at 405 nm was recorded every 30 s for 20 minutes by a microplate reader (Tecan Spark 10M, Männedorf, Switzerland). Acarbose was used as a positive control. The enzymatic activity without a sample was defined as 100%. The relative enzymatic activity was calculated based on the following equation 1 (Equation (1))

$$\text{The relative enzymatic activity (\%)} = \frac{R}{R_0} \times 100\% \tag{1}$$

where R and R_0 are the slopes of the linear part of the reaction kinetics obtained with the presence or absence of hesperidin, respectively. The half inhibitory concentration (IC_{50}) means the concentration of samples causing a loss of 50% enzymatic activity.

2.3. Kinetic Analysis of Enzyme Inhibition

The inhibition kinetic analysis was investigated by the same procedure as that described for the in vitro α-glucosidase inhibition assay. For the reversibility test, the concentration of substrate *p*NPG was kept at 4 mM, while the hesperidin concentration was set to 0, 6.14, 12.28, 1.38, and 20.47 x 10^{-5} M, respectively. The plot of velocity of enzymatic reaction *versus* α-glucosidase concentration with the presence of different concentration of hesperidin, was constructed to determine the reversibility of the inhibitor. For the inhibition type test, the α-glucosidase concentration was kept at 0.96 μM, while the concentration of hesperidin was set to 0, 6.14, 12.28, 1.38, and 20.47 x 10^{-5} M, respectively. Lineweaver-Burk plots were then constructed by the reciprocal velocity *versus* the reciprocal substrate concentration with the presence of different concentration of hesperidin. The values of the Michaelis-Menten constant (K_m) and the maximum velocity (V_{max}) were determined by the Lineweaver–Burk plots according to Equation (2) [18]. The values of new kinetic constants K_{ik} and K_{iv} which reflected the changes of K_m and V_{max} in responsible to the inhibitor concentrations were obtained by the Equations (3) and (4), respectively, based on Yang's method [19].

$$\frac{1}{V} = \frac{K_m}{V_{max}} \frac{1}{[S]} + \frac{1}{V_{max}} \tag{2}$$

$$\frac{1}{K_m} = \frac{1}{K_{m,0}} \text{ x} \left(1 + \frac{[I]}{K_{ik}}\right) \tag{3}$$

$$\frac{1}{V_{max}} = \frac{1}{V_{max,0}} \text{ x} \left(1 + \frac{[I]}{K_{iv}}\right) \tag{4}$$

where $V_{max,0}$ and $K_{m,0}$ are the maximum velocity and the Michaelis-Menten constant of the enzyme with the absence of an inhibitor, respectively. [S] and [I] represent the
concentrations of the substrate *p*NPG and the inhibitor hesperidin, respectively.

2.4. Fluorescence Spectroscopic Analysis

A fluorescence quenching experiment was used to investigate the interaction between α-glucosidase enzyme and hesperidin based on the methodology of He et al [7]. Different amounts of stock solution (25 mM in dimethyl sulfoxide) of hesperidin were titrated into a 3 mL α-glucosidase enzyme solution (0.96 μM) to achieve a series of final concentration of 0.55, 1.09, 2.19, 3.28, 4.37, 5.46 x 10^{-5} M for hesperidin, respectively. The corresponding enzyme solution without the addition of hesperidin was used as a blank control. At each concentration after the titration of hesperidin, the intrinsic fluorescence of the α-glucosidase enzyme was scanned by using a fluorescence spectrophotometer at a wavelength of 300-500 nm after being excited at 280 nm. The emission and excitation slit width was set to 2.5 nm. The fluorescence spectra were recorded at three different temperatures (298, 304, and 310 K). All fluorescence data were corrected to deduct the internal filtering effect caused by the ultraviolet absorption based on the following Equation (5) [7].

$$F_{\text{corr}} = F_{\text{obs}}e^{\frac{(A_1+A_2)}{2}} \hspace{3cm} (5)$$

where F_{corr} and F_{obs} represent the corrected and observed fluorescence intensities, respectively. A_1 and A_2 represent the absorbance of the corresponding solution at excitation and emission wavelength, respectively.

2.5. Molecular Docking

The molecular model of α-glucosidase (PDB ID: 7kad) was obtained from Protein Data Ban (https://www1.rcsb.org/). The 3D structure of hesperidin (compound CID: 10621) was derived from PubChem (https://pubchem.ncbi.nlm.nih.gov/) Database. The obtained molecular model of α-glucosidase was preprocessed using Autodock Tools 1.5.7 software to remove water, add hydrogen atoms, and perform charge calculation. The molecular docking calculation was performed using Auto Dock vina 1.2.3 software. The exhaustiveness parameter was set to 16 during the docking process while other parameters were kept as default values of the software. The binding mode with the lowest energy was selected as the most favorable conformation for further analysis. The molecular docking results were visualized and analyzed using both PyMol 2.6 and LigPlus software [20].

2.6. Statistical Analysis

All the experimental results were collected based on triplicate assay and the mean ± standard deviations error were recorded. The data were analyzed by one-way analysis of variance (ANOVA) using the SPSS (Version 6.0) statistical package at $P < 0.05$.

3. Results and Discussions

3.1. In Vitro Antidiabetic Effect of Hesperidin on α-Glucosidase Enzyme

Hesperidin was a flavonoid glycoside containing one glucose and one rhamnose as its subunits (Figure 1A), which was abundantly present in orange fruits [13]. In the present study, the inhibitory effect of hesperidin on α-glucosidase was assessed biochemically. As shown in Figure 1B, the enzymatic activity of α-glucosidase was significantly inhibited by hesperidin and the relative activity was gradually reduced along with the increase of hesperidin concentration, showing a dose-dependent manner. The enzymatic activity was almost completely inhibited when the hesperidin concentration was over 200 μM. The IC$_{50}$ value of hesperidin on enzyme inhibition was found to be 18.52 ± 1.26 μM based on the dose-activity curve, which was in line with a previous report showing the IC$_{50}$ of 15.75 μg/mL (25.8 μM) [17]. Interestingly, the inhibitory effect of hesperidin was comparable to the positive control Acarbose (IC$_{50}$ 12.24 μM), indicative of the great application potential of hesperidin as a substituent for Acarbose. Flavonoids are natural compounds widely present in plants and they possess immense biological value in terms of antioxidant, anticancer and antidiabetic properties [21,22]. Citrus plant-contained flavonoids like hesperidin, naringin, and nobiletin are proven to be effective against many metabolic disorders like hypertension and cardiovascular disease [23]. In an earlier finding, it was observed that hesperidin exhibited a selective and significant α-glucosidase inhibitory effect and also reduced the glucose-6-phosphate enzyme activity in HepG2 cells [24]. It is also proven that drinking orange juice consecutively reduces the postprandial blood glucose level which is associated with the hesperidin content of orange juice [25].
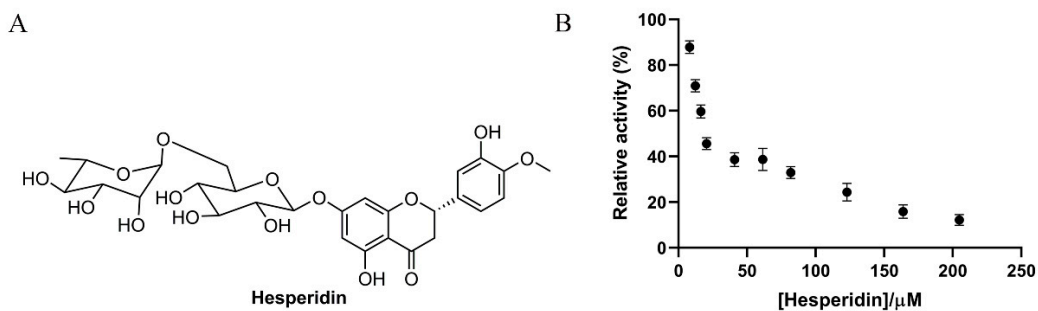
Figure 1. (A) Chemical structure of hesperidin. (B) Effect of different concentrations of hesperidin on the relative activity of α-glucosidase.

3.2. Kinetic Analysis of Enzyme Inhibition

The reversibility of the inhibitory effect was investigated by the plot of α-glucosidase concentration ([α-glucosidase]) *versus* the velocity (V) of the enzymatic reaction. As shown in Figure 2A, the velocity gradually increased along with the increase of the enzyme concentration at the same concentration of hesperidin. Meanwhile, all lines passed through the origin with good linearity and the slope decreased with the increase of hesperidin concentration. These results indicated that α-glucosidase was not completely inactivated, but the catalytic rate of the enzyme was decreased by hesperidin, suggesting that hesperidin was a reversible inhibitor against α-glucosidase enzyme according to previous studies [18,26]. It was reported that irreversible inhibitors completely inactivated enzymes by forming stable complexes via covalent intermolecular interactions [27]. Furthermore, the Line-weaver-Burk double-reciprocal plot was used to determine the inhibition type of hesperidin on α-glucosidase. As shown in Figure 2B, a family of parallel lines was obtained by plotting 1/V against 1/[pNPG], suggestive of the type of uncompetitive inhibition [18]. Meanwhile, as shown in Table 1, both the K_m and V_{max} values acquired from the Equation (2) gradually decreased with the increase of hesperidin concentration, which was in line with the uncompetitive inhibition kinetics of cinnamic acid amide on α-glucosidase [28]. To further confirm the uncompetitive inhibition type of hesperidin on α-glucosidase, two new kinetic constants K_{ik} and K_{iv} were calculated from the Equations (3) and (4). According to Yang's method, the ratio of K_{iv}/K_{ik} below 2.0 suggests that the inhibition is an uncompetitive type, over 5.0 implies noncompetitive or competitive, and from 2.0 to 5.0 indicates a mixed-type inhibition [19]. As shown in Table 1, the ratio of K_{iv}/K_{ik} was around 1.0 at different concentrations of hesperidin, which was indicative of an uncompetitive inhibition. Natural products as uncompetitive inhibitors of α-glucosidase have not been reported much so far [5]. The only a few examples reported previously include vitexin [29], corosolic acid [18], cinnamic acid amide [28], and ginsenoside Rg1 [30]. The present discovery of hesperidin as an excellent uncompetitive inhibitor should be very interesting since this type of inhibitor was generally more efficient than competitive and noncompetitive inhibitors for the in vivo assay [31].

Table 1. Effect of different concentrations of hesperidin on V_{max}, K_m of α-glucosidase, and ratios of the K_{iv} to K_{ik} using pNPG (p-nitrophenyl-α-D-glucopyranoside) as substrate.

[I](hesperidin)/μM	V_{max}	K_m	K_{iv}/K_{ik}
0	0.29	6.70	//
61.42	0.10	2.44	0.92
122.84	0.04	0.91	1.02
163.78	0.03	0.90	0.96
201.73	0.02	0.46	1.01
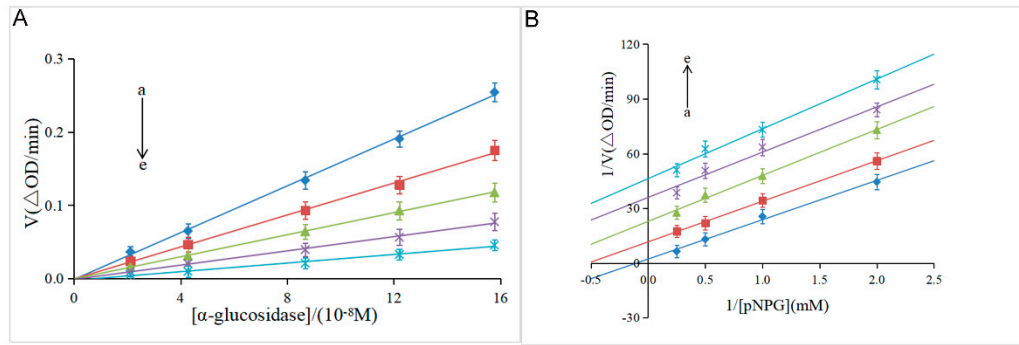
Figure 2. (A) Plots of V versus [α-glucosidase]. [pNPG] = 4 mM, [hesperidin] = 0, 6.14, 12.28, 16.38，20.47×10⁻⁵M for curves a→e, respectively. (B) Lineweaver-Burk plots. [α-glucosidase] = 0.96 μM, [hesperidin] = 0, 6.14, 12.28, 16.38, 20.47×10⁻⁵M for curves a→e, respectively.

3.3. Fluorescence Quenching Assay

The intrinsic fluorescence of α-glucosidase is mainly attributable to the presence of Trp (Tryptophan) and Tyr (tyrosine) residues which emit fluorescence at the excitation wavelength of 280 nm [18]. Figure 3A depicted clearly that in the presence of only α-glucosidase, the highest emission peak was at 345 nm when the excitation wavelength was 280 nm, which was in good agreement with previous reports [29,30]. Hesperidin had no interference on α-glucosidase fluorescence because hesperidin did not show any signal under the same conditions (curve h of Figure 3A). The fluorescence of α-glucosidase was gradually quenched with increasing hesperidin concentration (curves a-g, Figure 3A), suggesting that the conformation of the enzyme might be modified due to the interaction between hesperidin and α-glucosidase. The Stern-Volmer equation (Equation (6)) was then applied to investigate the quenching mechanism of α-glucosidase by hesperidin.

$$\frac{F_0}{F} = 1 + K_{sv}[Q] = 1 + K_q \tau_0 [Q] \tag{6}$$

In the above formula, F and F_0 represent the corrected fluorescence intensity of α-glucosidase in the presence and absence of the inhibitor, respectively; [Q] is the concentration of the inhibitor; K_{sv} and K_q represent the quenching constant and bimolecular quenching rate constant, respectively; τ_0 represents the fluorophore lifetime of a free biomacromolecule, which is approximately 10⁻⁸ s for α-glucosidase [32].
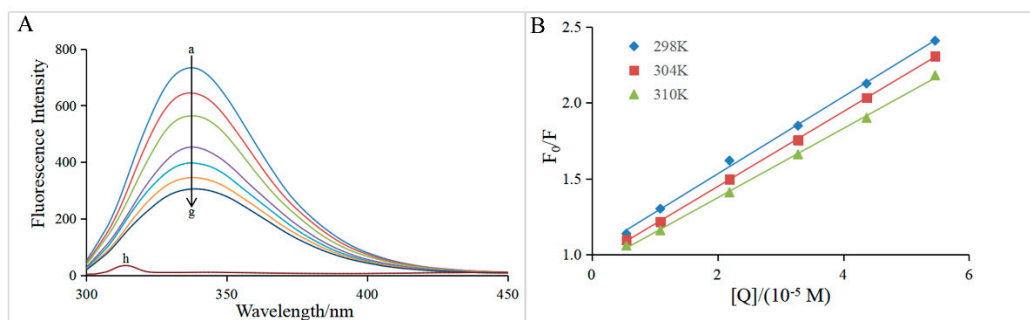

Figure 3. (A) Fluorescence spectra of α-glucosidase in the presence of various concentrations of hesperidin. T = 298 K, λ_{ex} = 280 nm, [α-glucosidase] = 0.96 μM，[hesperidin] = 0, 0.55, 1.09, 2.19, 3.28, 4.37, 5.46×10⁻⁵M for curves a→g, respectively. Curve h shows the emission spectrum of hesperidin at the concentration of 0.55×10⁻⁵ M. (B) The Stern-Volmer plots at three different temperatures (T = 298, 304, 310 K).

As shown in Figure 3B, the plot of F_0/F *versus* [Q] exhibited good linearity at all three different temperatures (298, 304, and 310 K), indicating that the quenching process by hesperidin was a single

static or dynamic quenching [33]. The slope of the straight line represented the K_{SV} value at the corresponding temperature, and the K_{SV} values at all three temperatures were listed in Table 2. The K_{SV} value decreased with the increase in temperature, which was a characteristic of the static quenching process [34]. In addition, all the corresponding K_q values were of the 10^{12} magnitude order, which was much larger than the maximum diffusion collision quenching rate constant of biological macromolecules (2.0×10^{10} L mol^{-1}s^{-1}), further confirming that the quenching process of α-glucosidase by hesperidin was a static quenching [29,35]. The present result suggested the fluorescence quenching by hesperidin should be achieved via the formation of a ground-state complex rather than a dynamic collision process.

Table 2. The quenching constant (K_{SV}), binding constant (K_a), number (n) of binding site, and thermodynamic parameters of hesperidin α-glucosidase complex at three different temperatures.

T (K)	K_{SV} ($\times 10^5$ L mol^{-1})	K_a ($\times 10^4$ L mol^{-1})	n	ΔH^o (kJ mol^{-1})	ΔG^o (kJ mol^{-1})	ΔS^o (J mol^{-1} K^{-1})
298	2.58±0.01a	2.97±0.04a	1.07±0.05a		-25.51±0.03a	
304	2.40±0.05b	2.44±0.25b	1.06±0.01a	-22.82±2.06	-25.56±0.02a	9.03±0.08
310	2.11±0.18c	2.08±0.17c	0.96±0.04a		-25.62±0.02a	

Data are presented as mean ± SD (n = 3). Different lowercase letters following the data within the same column indicate significant statistical difference ($p < 0.05$).

By using the fluorescence quenching data, the binding constant (K_a) and the number (n) of the binding site were obtained as well based on Equation (7) [36], where the [P_t] and [Q_t] were the concentrations of α-glucosidase and hesperidin, respectively.

$$\log\frac{F_0 - F}{F} = n\log K_a - n\log \frac{1}{[Q_t] - \frac{(F_0 - F)[P_t]}{F_0}} \tag{7}$$

According to Equation (7), the values of K_a at 298, 304 and 310 K were calculated. As shown in Table 2, all K_a values had a magnitude order of 10^4 L mol^{-1}, suggesting a strong binding affinity between α-glucosidase and hesperidin [29]. In addition, it can be seen from the data in Table 2 that the K_a value decreased with the increase in reaction temperature, indicating that the stability of the inhibitor-enzyme complex decreased with the increase in temperature, and this result further confirmed that the fluorescence quenching by hesperidin was a static process. Furthermore, the n values (1.07, 1.06, and 0.96) obtained at three different temperatures were all close to 1 (Table 2), suggesting that there was only one binding site between hesperidin and α-glucosidase [18,37].

To further identify the driving forces for the formation of the α-glucosidase-hesperidin complex, the thermodynamic parameters involving enthalpy change ($\Delta H°$), entropy change ($\Delta S°$), and the Gibbs free energy ($\Delta G°$) of the binding process were calculated according to the Equations (8) and (9) (van't Hoff equation), where R is the gas constant (8.314 J mol^{-1}K^{-1}), and K_a denotes the binding constant at the corresponding temperature.

$$\log K_a = -\frac{\Delta H^0}{2.303RT} + \frac{\Delta S^0}{2.303RT} \tag{8}$$

$$\Delta G^0 = \Delta H - T\Delta S^0 \tag{9}$$

In the present study, since the variation range of the temperature was narrow, the enthalpy change ($\Delta H°$) can be considered as a constant [6]. The main non-covalent interactions between enzymes and inhibitors include electrostatic interaction, hydrophobic forces, hydrogen bonds, and van der Waals forces. As shown in Table 2, the $\Delta G°$ of the present study was around -25 KJ mol^{-1} at all three temperatures, less than zero ($\Delta G° < 0$), indicating that the binding of hesperidin with α-glucosidase was a spontaneous procedure [27]. Furthermore, $\Delta H° < 0$ and $\Delta S° > 0$ (Table 2) suggested that the dominant driving forces for the binding procedure of hesperidin with α-glucosidase were hydrogen bonds and hydrophobic interactions [29,38].

3.4. Molecular Docking

Molecular docking was used to further determine the interaction between α-glucosidase and hesperidin (Figure 4). The lowest binding energies of the α-glucosidase-hesperidin complex was -11.375 kcal/mol, indicating that the interaction between α-glucosidase and hesperidin was strong and occurred spontaneously, which was in line with the result of the thermodynamic investigation showing $\Delta G° < 0$. As shown in Figure 4B, hesperidin formed five hydrogen bonds with the amino acid residues involving Trp709, Arg422, Asn424, and Arg467 with the distance ranging from 2.3 to 2.9 Å. Moreover, hesperidin was surrounded by a serial of amino acid residues such as Asp430, Arg705, Glu707, Arg426, Arg467, Trp423, and Asn424 via hydrophobic forces (Figure 4C). These observations indicated that hydrogen bonds and hydrophobic forces were the main driving forces between hesperidin and α-glucosidase, which was in good agreement with the results of thermodynamic analysis. Many previous studies have reported that amino acid residues involving Tyr 158, Phe 159, Asp 215, Glu 277, Arg 312, Asp 352, and Glu 411 play critical roles in binding substrate, and they might form an enzymatically active site of α-glucosidase [39,40]. The present docking study indicated that hesperidin bound to sites other than the active center of α-glucosidase, which was consistent with the results obtained in the kinetic analysis showing that hesperidin was an uncompetitive inhibitor. As an uncompetitive inhibitor, hesperidin only binds with the enzyme-substrate complexes, showing no competition to the active center of the enzyme. Therefore, the present results allowed us to propose that the hesperidin might bond to the entrance or outlet part of the active center, thereby obstructing the release of the substrate and catalytic reaction product from the active center, eventually inhibiting the enzymatic activity of α-glucosidase. Similarly, uncompetitive inhibitors like cinamic acid amide [28], corosolic acid [18], and ginsenoside Rg1 [30] were suggested to bond to the entrance of the active center of α-glucosidase based on the results of molecular docking studies.
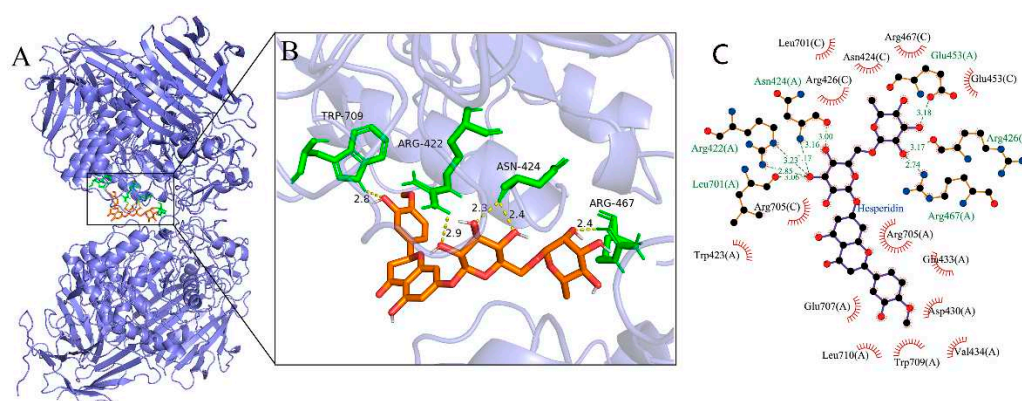

Figure 4. (A) Molecular simulation diagram of hesperidin α-glucosidase complex. (B) The hydrogen bonds between hesperidin and α-glucosidase. (C) The hydrophobic interactions formed between hesperidin and α-glucosidase.

4. Conclusions

The present research elucidated the inhibitory mechanism of hesperidin on α-glucosidase through enzyme kinetics, thermodynamics, and molecular modeling approach for the first time. Hesperidin was found to exhibit a significant inhibitory effect on the enzymatic activity of α-glucosidase through a reversible and uncompetitive inhibition mode. Fluorescence quenching results indicated that hesperidin spontaneously bonded to α-glucosidase with one binding site by non-covalent interactions which mainly consisted of hydrogen bonds and hydrophobic effects. Molecular docking studies suggested that hesperidin might bond to the entrance or outlet part of the active center of the enzyme, thus blocking the release of substrate and catalytic product. The result revealed here gave an insight into the inhibitory mechanism of hesperidin on α-glucosidase, supporting the

application potential of orange fruits which are rich in hesperidin, as an anti-hyperglycemic agent. Further research on in vivo experiments would be much more supportive of the antidiabetic effect of hesperidin.

References

1. Wang, J.; Liu, F.; Kong, R.; Han, X. Association between globulin and diabetic nephropathy in type2 diabetes mellitus patients: a cross-sectional study. *Front. Endocrin.* **2022**, *13*, 890273.
2. Schalkwijk, C.G.; Stehouwer, C.D.A. Methylglyoxal, a highly reactive dicarbonyl compound, in diabetes, its vascular complications, and other age-related diseases. *Physiol. Rev.* **2020**, *100*, 407-461.
3. Bonora, E.; Muggeo, M. Postprandial blood glucose as a risk factor for cardiovascular disease in type II diabetes: the epidemiological evidence. *Diabetologia*, **2001**, *44*, 2107-2114.
4. Toeller, M. α-Glucosidase inhibitors in diabetes: efficacy in NIDDM subjects. *Eur. J. Clin. Invest.* **1994**, *24*, 31-35.
5. Tundis, R.; Loizzo, M.R.; Menichini, F. Natural products as α-amylase and α-glucosidase inhibitors and their hypoglycaemic potential in the treatment of diabetes: an update. *Mini. Rev. Med.Chem.* **2010**, *10*, 315-331.
6. Fan, Y.; Tao, Y.; Wang, S.; Wang, M.; Li, L. Inhibitory interaction of narcissoside on α-glucosidase from *Aspergillus niger* and *Saccharomyces cerevisiae* by spectral analysis and molecular docking. *J. Molec. Struc.* **2022**, *1264*, 133262.
7. He, M.; Zhai, Y.; Zhang, Y.; Xu, S.; Yu, S.; Wei, Y.; Song, Y. Inhibition of α-glucosidase by trilobatin and its mechanism: kinetics, interaction mechanism and molecular docking. *Food. Func.* **2022**, *13*, 857-866.
8. Tian, J.L.; Zhao, M.; Xu, J.Y.; Lv, T.M.; Liu, X.C.; Sun, S.; Hu, P. Inhibitory Mechanism of Prenylated Flavonoids Isolated from Mulberry Leaves on α-Glucosidase by Multi-Spectroscopy and Molecular Dynamics Simulation. *J. Agri. Food Chem.* **2023**, *71*, 9135-9147.
9. Vergine, M.; Nicolì, F.; Sabella, E.; Aprile, A.; De Bellis, L.; Luvisi, A. Secondary metabolites in *Xylella fastidiosa*–plant interaction. *Pathogens* **2020**, *9*, 675.
10. Roohbakhsh, A.; Parhiz, H.; Soltani, F.; Rezaee, R.; Iranshahi, M. Molecular mechanisms behind the biological effects of hesperidin and hesperetin for the prevention of cancer and cardiovascular diseases. *Life Sci.* **2015**,*124*, 64-74.
11. Ullah, A.; Munir, S.; Badshah, S.L.; Khan, N.; Ghani, L.; Poulson, B.G.; Jaremko, M. Important flavonoids and their role as a therapeutic agent. *Molecules* **2020**, *25*, 5243.
12. Zhang, Z.; Li, X.; Sang, S.; McClements, D.J.; Chen, L.; Long, J.; Qiu, C. Polyphenols as plant-based nutraceuticals: health effects, encapsulation, nano-delivery, and application. *Foods* **2022**, *11*, 2189.
13. Zhang, L.; Ling, W.; Yan, Z.; Liang, Y.; Guo, C.; Ouyang, Z.; Zhang, J. Effects of storage conditions and heat treatment on the hesperidin concentration in Newhall navel orange (*Citrus sinensis* Osbeck cv. Newhall) juice. *J. Food. Compo. Anal.* **2020**, *85*, 103338.
14. Guo, C.; Shan, Y.; Yang, Z.; Zhang, L.; Ling, W.; Liang, Y.; Zhang, J. Chemical composition, antioxidant, antibacterial, and tyrosinase inhibition activity of extracts from Newhall navel orange (*Citrus sinensis* Osbeck cv. Newhall) peel. *J. Sci. Food Agri.* **202**0, *100*, 2664-2674.
15. Xiong, H.; Wang, J.; Ran, Q.; Lou, G.; Peng, C.; Gan, Q.; Hu, J.; Sun, J.; Yao, R.; Huang, Q. Hesperidin: A therapeutic agent for obesity. Drug. Des. Develop. Ther. **2019**, *13*, 3855-3866.
16. Loizzo, M.R.; Falco, T.; Bonesi, M. *Ruta chalepensis* L. (Rutaceae) leaf extract: chemical composition, antioxidant and hypoglycaemic activities. Nat. Prod. Res. **2018**, *32*, 521-528.
17. Zhang, J.; Zhang, L.; Lai, C.; Liang, Y.; Gao, L.; Kaliaperumal, K.; Jiang, Y. Nutraceutical potential of navel orange peel in diabetes management: The chemical profile, antioxidant, α-glucosidase inhibitory and antiglycation effects of its flavonoids. *Food Biosci.* **2022**, *49*, 101943.
18. Ni, M.; Pan, J.; Hu, X.; Gong, D.; Zhang, G. Inhibitory effect of corosolic acid on α-glucosidase: kinetics, interaction mechanism, and molecular simulation. *J. Sci. Food Agri.* **2019**, *99*, 5881-5889.

19. Yang, X.; Du, Z.; Pu, J.; Zhao, H.; Chen, H.; Liu, Y.; Liao, F. Classification of difference between inhibition constants of an inhibitor to facilitate identifying the inhibition type. *J. Enz. Inhib. Med. Chem.* **2013**, *28*, 205-213.

20. Laskowski, R.A.; Swindells, M.B. LigPlot+: multiple ligand-protein interaction diagrams for drug discovery. J. Chem. Inf. Model **2011**, *51*, 2778-2786.

21. Karak, P. Biological activities of flavonoids: An overview. *Int. J. Pharm. Sci. Res.* **2019**, *10*, 1567-1574.

22. Wang, Z.; Tu, Z.; Xie, X.; Cui, H.; Kong, K.W.; Zhang, L. *Perilla frutescens* leaf extract and fractions: polyphenol composition, antioxidant, enzymes (α-glucosidase, acetylcholinesterase, and tyrosinase) inhibitory, anticancer, and antidiabetic activities. *Foods* **2021**, *10*, 315.

23. Alam, F.; Mohammadin, K.; Shafique, Z.; Amjad, S.T.; Asad, M.H.H.B. Citrus flavonoids as potential therapeutic agents: A review. *Phytother. Res.* **2022**, *36*, 1417-1441.

24. Shen, W.; Xu, Y.; Lu, Y.H. Inhibitory effects of citrus flavonoids on starch digestion and anti-hyperglycemic effects in HepG2 cells. *J. Agri. Food Chem.* **2012**, *26*, 9609-9619.

25. Kerimi, A.; Gauer, J.S.; Crabbe, S.; Cheah, J.W.; Lau, J.; Walsh, R.; Williamson, G. Effect of the flavonoid hesperidin on glucose and fructose transport, sucrase activity and glycaemic response to orange juice in a crossover trial on healthy volunteers. *Brit. J. Nut.* **2019**, *121*, 782-792.

26. Zeng, L.; Ding, H.; Hu, X.; Zhang, G.; Gong, D. Galangin inhibits α-glucosidase activity and formation of non-enzymatic glycation products. *Food Chem.* **2019**, *271*, 70-79.

27. Zeng, L.; Zhang, G.; Lin, S.; Gong, D. Inhibitory mechanism of apigenin on α-glucosidase and synergy analysis of flavonoids. *J. Agri. Food Chem.* **2016**, *64*, 6939-6949.

28. Song, Y.H.; Kim, D.W.; Curtis-Long, M.J.; Park, C.; Son, M.; Kim, J. Y.; Park, K.H. Cinnamic acid amides from *Tribulus terrestris* displaying uncompetitive α-glucosidase inhibition. *Eur. J. Med. Chem.* **2016**, *114*, 201-208.

29. Ni, M.; Hu, X.; Gong, D.; Zhang, G. Inhibitory mechanism of vitexin on α-glucosidase and its synergy with acarbose. *Food Hydrocoll.* **2020**, *105*, 105824.

30. Liu, Y.; Zhang, J.; An, C.; Liu, C.; Zhang, Q.; Ding, H.; Fan, D. Ginsenoside Rg1 alleviates the postprandial blood glucose by inhibiting α-glucosidase. *J. Funct. Foods* **2023**, *107*, 105648.

31. Cornish-Bowden, A. Why is uncompetitive inhibition so rare?: A possible explanation, with implications for the design of drugs and pesticides. *FEBS Lett*. **1986**, *203*, 3-6.

32. Shu, Y.; Xue, W.; Xu, X.; Jia, Z.; Yao, X.; Liu, S.; Liu, L. Interaction of erucic acid with bovine serum albumin using a multi-spectroscopic method and molecular docking technique. *Food Chem.* **2015**, *173*, 31-37.

33. Yang, Y.; Zhang, P; Huang, Z.; Zhao, Z. Phenolics from *Sterculia nobilis* Smith pericarp by-products delay carbohydrate digestion by uncompetitively inhibiting α-glucosidase and α-amylase. *LWT* **2023**, *173*, 114339.

34. Li, Y.Q.; Zhou, F.C.; Gao, F.; Bian, J.S.; Shan, F. Comparative evaluation of quercetin, isoquercetin and rutin as inhibitors of α-glucosidase. *J. Agri. Food Chem.* **2009**, *57*, 11463-11468.

35. Maurya, N.; ud din Parray, M.; Maurya, J.K.; Kumar, A.; Patel, R. Interaction of promethazine and adiphenine to human hemoglobin: A comparative spectroscopic and computational analysis. *Spectrochim. Acta. Part A: Mol. Biomol. Spectro.* **2018**, *199*, 32-42.

36. Wu, X.; Ding, H.; Hu, X.; Pan, J.; Liao, Y.; Gong, D.; Zhang, G. Exploring inhibitory mechanism of gallocatechin gallate on α-amylase and α-glucosidase relevant to postprandial hyperglycemia. *J. Funct. Foods* **2018**, *48*, 200-209.

37. Dohare, N.; Khan, A.B.; Maurya, N.; Thakur, S.; Athar, F.; Singh, P.; Patel, R. An insight into the binding of aceclofenac with bovine serum albumin at physiological condition: a spectroscopic and computational approach. *J. Biomol. Struct. Dynam.* **2018**, *36*, 398-406.

38. Dai, T.; Chen, J.; McClements, D.J.; Hu, P.; Ye, X.; Liu, C.; Li, T. Protein–polyphenol interactions enhance the antioxidant capacity of phenolics: Analysis of rice glutelin–procyanidin dimer interactions. *Food Funct.* **2019**, *10*, 765-774.

39. Zhang, H.; Xu, C.; Tian, Q.; Zhang, Y.; Zhang, G.; Guan, Y.; Yan, J. Screening and characterization of aldose reductase inhibitors from Traditional Chinese medicine based on ultrafiltration-liquid chromatography mass spectrometry and in silico molecular docking. *J. Ethnopharmacol.* **2021**, *264*, 113282.

40. Shen, H.; Wang, J.; Ao, J.; Cai, Y.; Xi, M.; Hou, Y.; Li, M.; Luo, A. Inhibitory kinetics and mechanism of active compounds in green walnut husk against α-glucosidase: Spectroscopy and molecular docking analyses. *LWT* **2022**, *172*, 114179.